

perimental data prior to publication and to Professor F. Jelinek for several helpful comments regarding bulk Ni-S compounds.

¹S. Andersson and J. B. Pendry, *J. Phys. C: Proc. Phys. Soc.*, London **5**, 41 (1972).

²J. E. Demuth, P. M. Marcus, and D. W. Jepsen, in *Proceedings of the Seventh Low-Energy Electron Diffraction Symposium*, San Diego, California, March 1973 (to be published).

³G. E. Laramore, *Phys. Rev. B* **8**, 515 (1973).

⁴J. E. Demuth, D. W. Jepsen, and P. M. Marcus, *Phys. Rev. Lett.* **31**, 540 (1973).

⁵J. E. Demuth, D. W. Jepsen, and P. M. Marcus, *Solid State Commun.* **13**, 1311 (1973).

⁶J. E. Demuth, D. W. Jepsen, and P. M. Marcus, to

be published.

⁷H. D. Hagstrum and G. E. Becker, *Surface Sci.* **30**, 505 (1972).

⁸M. Perdereau and J. Oudar, *Surface Sci.* **20**, 80 (1970).

⁹D. W. Jepsen, P. M. Marcus, and F. Jona, *Phys. Rev. B* **6**, 3864 (1972).

¹⁰S. Wakoh, *J. Phys. Soc. Jap.* **20**, 1984 (1965).

¹¹J. E. Demuth and T. N. Rhodin, to be published.

¹²F. Forstman, W. Berndt, and P. Buttner, *Phys. Rev. Lett.* **30**, 17 (1973).

¹³W. R. Graham and G. Ehrlich, *J. Chem. Phys.* **59**, 3417 (1973).

¹⁴L. Pauling, *The Nature of the Chemical Bond* (Cornell Univ. Press, New York, 1964).

¹⁵S. G. Gmelin, *Handbuch der Anorganischen Chemie* (Verlag Chemie, Weinheim/Bergstrasse, Germany, 1966), Vol. 57, Part 2, p. 657.

Direct Evidence of Pretransformation Lattice Instabilities

H. C. Tong and C. M. Wayman

Department of Metallurgy and Mining Engineering and Materials Research Laboratory, University of Illinois at Urbana-Champaign, Urbana, Illinois 61801

(Received 11 March 1974)

Observations on lattice instability are demonstrated by transmission and diffraction electron microscopy together with an electron multiplier. The latter displays the coupled atomic fluctuations on an oscilloscope screen. The WKB method has been used to calculate a single-atom transition time. The results indicate that fluctuations should be present and that quantum mechanical considerations are important in the nucleation of solid-state phase transformation. A standing-wave model is suggested for the pretransition lattice instabilities and is experimentally supported.

A number of alloys undergoing phase transitions apparently exhibit soft phonon modes when cooled to a temperature approaching the critical temperature for the structural transition. Of recent interest have been the alloys V_3Si and Nb_3Sn .¹ At high temperatures, these materials possess the β -tungsten structure, but at lower temperatures they undergo a cubic-to-tetragonal martensitic transition. These alloys are reported to exhibit the superconducting state a few degrees below the martensite start temperatures ($M_s = 22$ and $43^\circ K$, respectively, for V_3Si and Nb_3Sn). In addition, the elastic anisotropy factor $A = 2C_{44}/(C_{11} - C_{12})$ is large for these materials near the transition temperature, which indirectly indicates a lattice softening behavior. The observed lattice instability has been viewed as a band Jahn-Teller effect.² However, it should be noted that Au-Cd,³ Au-Cu-Zn,⁴ and In-Tl alloys⁵ also undergo martensitic transformations and show a large

elastic anisotropy near the M_s temperature. It has been noted especially that $C_{11} - C_{12} \rightarrow 0$ as $T \rightarrow M_s$ for β -Au-Cu-Zn alloys.⁴ Since not all of these alloys are based on transition elements and none exhibits the β -tungsten structure, the universal importance of the Jahn-Teller interpretation can be questioned. However, certain common characteristics apply to the previous alloys: All undergo structural phase transitions without compositional change, and as the transformation proceeds, the product phase is "connected" to the parent in a highly coherent manner, typical of thermoelastic martensitic transformations. Since Cu-Zn,⁶ Ag-Cd,⁷ Ni-Ti,⁸ Fe-Pt,⁹ Cu-Au,¹⁰ Fe-Ni,¹¹ and other alloys have the same common characteristics, lattice instabilities in these cases might also be expected.

The direct observation of lattice instabilities can be made by studying the *in situ* transformation process and kinetics with a controllable heat-

ing and cooling electron microscope stage and provisions for ciné film recording.¹² In addition to this, an electron multiplier has been employed to detect the lattice instabilities. The multiplier was mounted directly below a 0.020-in. hole drilled through the fluorescent screen of the electron microscope. The typical current flux through this aperture and into the multiplier was about 10^{-12} A. The multiplier output showed the lattice instabilities to be presented in a dynamic fluctuating manner. At a magnification of 20 000 to 50 000 times, the lattice oscillations were observed on the screen by the unaided eye, indicating at least that a part of the spectrum is very low frequency in nature.

Epitaxially grown (001) CuAu films prepared by rf sputtering were used as a typical example to describe the instability phenomenon. Although, formally, the fcc to CuAu II transition is an order-disorder transformation, it is considered to be martensitic in nature.^{10,13} In addition to martensitic crystallographic features, there is no composition change during this transformation.



FIG. 1. (a) Background noise from 100-keV electron beam and electron multiplier. (b) Fluctuations in electron multiplier signal which correspond to pretransformation phenomena. The electron current input is the same as for (a) and the horizontal scale is 0.2 sec/cm. (c) Electron micrograph showing streaminglike lattice oscillations in CuAu alloy during pretransformation period.

Above the critical temperature, $T_c = 410^\circ\text{C}$, the *in situ* electron microscope observations showed that the observed fluctuations were highly orientation (Bragg contrast) dependent. When in strong contrast, the fluctuating image invariably appeared as a domainlike network on the order of 100 \AA in size. The domains go in and out of contrast relative to each other in a dynamic manner. Within a given area of observation, the fluctuations detected by the electron multiplier were recorded on an oscilloscope screen as shown in Figs. 1(a) and 1(b). The overall image appears to shimmer like a streaming flow of water as shown in Fig. 1(c).

The lattice fluctuations were found to start about $50\text{--}60^\circ\text{C}$ above T_c , and the severity (observability) was increased as T_c was approached. Above T_c , the effect was time independent and the fluctuations did not die off. When the temperature was reduced from $T > T_c$ to slightly below T_c , the fluctuations were initially detected, and a gridlike microstructure developed from the streaming pattern as shown in Fig. 2(a). The rectangular symmetry of the gridlike structure was in perfect correspondence with the $\langle 100 \rangle$ di-

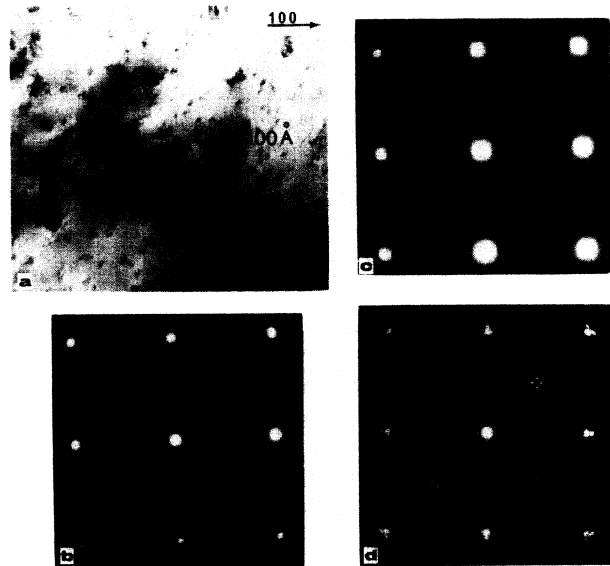


FIG. 2. (a) Transmission electron micrograph of CuAu thin film taken just before incipient transformation at 385°C (fcc \rightarrow CuAu II) showing the appearance of gridlike domain structure. (b) Diffraction pattern of CuAu film taken at 600°C showing sharp maxima. (c) Diffraction pattern of CuAu film taken at 385°C before transformation showing diffuse intensity and broadening of maxima caused by lattice oscillations. (d) Diffraction pattern of transformed CuAu thin film taken at 385°C showing sharp diffraction maxima.

rections of prominent streaming. After the initial lattice instabilities, large-scale nucleation and growth of the new phase occurred. The above phenomena were completely reproducible upon heating and cooling a given specimen. As a check against artifacts, similar observations were repeated using "dummy" (nontransforming) materials such as pure copper and nickel, in which cases the lattice oscillations were not observed.

Electron diffraction patterns also correspond with the fluctuations observed in the bright-field images. When the temperature was well above T_c the diffraction spots were very sharp. However, upon approaching T_c and at temperatures slightly below, the spots became highly broadened and showed diffuse intensities before the actual transformation began. The spots became sharp again after the transformation was completed. The highly diffuse and broadened reflections are taken to be additional evidence for the fluctuations as a consequence of the lattice instability. A typical sequence of diffraction spots is shown in Figs. 2(b)–2(d).

Since the atoms in a solid are not completely independent of their neighbors, lattice instabilities as observed in the present case are considered to be a result of a cooperative, coupled effect. Consequently, entire, localized lattice regions will produce a dynamical relaxation of the Bragg condition in a given small region of the specimen. This will result in significant inelastic (diffuse) scattering. Further, the diffraction contrast as seen in the electron microscope will fluctuate from place to place because of the dynamical Bragg relaxation.

It should also be pointed out that experiments on Fe-Ni⁶ and Ag-Cd alloys,¹² for example, also showed pretransformation lattice oscillations, and at low temperatures where thermal activation is not significant. In this regard, we consider a hypothetical cubic-tetragonal phase transition in which no composition change is involved. For example, a cubic unit cell is phenomenologically distorted into a corresponding tetragonal cell as shown in Fig. 3(a). The lattice potential curves for both phases are shown as a function of temperature in Fig. 3(b). At the temperature T_0 , where the potentials of an atom at D and D' are the same, two minima exist, which correspond to the equilibrium positions of atoms in the cubic and tetragonal unit cells [Figs. 3(a) and 3(b)].¹⁴ In general, the distance between neighboring minima will be on the order of 0.1 Å. For this separation, the uncertainty principle indi-

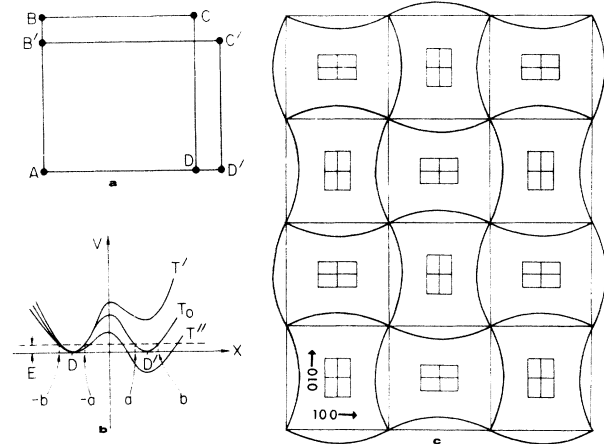


FIG. 3. (a) Schematic representation of hypothetical, two-dimensional cubic-tetragonal diffusionless phase transition. (b) Schematic representation of lattice potential $V(X)$ viewed by each atom in the crystal versus atomic position X [as in (a)] at different temperatures. (c) Large-scale long-standing-wave model depicting two-dimensional lattice instabilities. Note the alternation of tetragonality.

cates an energy uncertainty of about 0.005 eV relative to a typical activation barrier on the order of 0.1 eV.

The previous conditions being considered as representative, the WKB approximation was used to determine the parent-to-product transition time for a single atom at T_0 , assuming that a given atom is situated in a double-wall potential. Accordingly, the eigenenergy states are given by solution of the following equation:

$$\cot R_1 \cot R_2 = \exp(-2P), \quad (1)$$

where

$$R_1 = (1/\hbar) \int_{-b}^{-a} \{2m[E - V(x)]\}^{1/2} dx,$$

$$R_2 = (1/\hbar) \int_a^b \{2m[E - V(x)]\}^{1/2} dx,$$

$$P = (1/\hbar) \int_{-a}^a \{2m[V(x) - E]\}^{1/2} dx.$$

At $T = T_0$, the potential minima are equal, and furthermore if the double potential wall is assumed symmetrical (at T_0), Eq. (1) becomes

$$\cot R = \pm \frac{1}{2} \exp(-P) \quad (2)$$

and the energy separation of the two states is

$$\Delta E = (\hbar\omega/\pi) \exp(-P). \quad (3)$$

The time required for a transition between the parent and martensitic positions, for a single

atom, is then

$$\Delta\tau \sim (\pi/\omega) \exp(P). \quad (4)$$

If a cosine function is used to approximate the energy barrier of width L and height Q , Eq. (4) can be further simplified to

$$\Delta\tau = (\pi/\omega) \exp[(4L/h)(2mQ)^{1/2}]. \quad (5)$$

With reference to Eq. (5), taking $\omega = 6 \times 10^{13}/\text{sec}$, $L = 0.1 \text{ \AA}$, $m = 50 \text{ amu}$, and $Q = 0.1 \text{ eV}$, $\Delta\tau$ is found to be $\sim 10^{-12} \text{ sec}$. Such a very short single-atom transition time serves to emphasize that a large transition probability exists for realistic values of the displacement distance and energy barrier height. Thus, quantum mechanical aspects of the problem become important when considering the oscillation of atoms between two lattices, particularly at low temperatures where thermal activation is not significant. With reference to Eq. (3), the energy uncertainty is $\sim 10^{-2} \text{ eV}$. Thus, since the lattice atoms have a high transition probability for the hypothetical case presented, it is reasonable to regard the observed pretransformation effects as a natural consequence of a cooperative long-wave motion, as shown schematically in Fig. 3(c). It should be noted that the transition time for a single atom represents the upper limit for the formation of the new "phase" in the metastable, fluctuating parent. Values are expected to be lower for cooperative oscillations involving a number of atoms.

The long-wave model transforms cubic cells into tetragonal cells from one local region to another. However, since volume must be conserved, at least approximately, in order to minimize the accumulation of strain energy, it is envisioned that the sense of the tetragonality should oscillate periodically along $\langle 100 \rangle$ directions. Such an arrangement would lead naturally to a standing-wave pattern as shown in Fig. 3(c). The transmission electron microscope image taken immediately before transformation [Fig. 2(a)] shows a gridlike periodicity whose crystallography paral-

els the proposed model, and therefore provides good experimental justification.

In conclusion, we have presented direct evidence for pretransformation lattice instabilities which take the form of lattice fluctuations of a long-standing-wave nature. Although not explicitly observed, high-frequency lattice oscillations may also exist. However, at the present stage, noise from the electron microscope gun and the electron multiplier operating within the electron microscope under poor vacuum (10^{-5} Torr) preclude the detection of higher frequencies.

This work was supported by the U. S. Atomic Energy Commission through the Materials Research Laboratory at the University of Illinois.

¹K. R. Keller and J. J. Hanak, Phys. Rev. **154**, 628 (1967).

²E. Pytte, Phys. Rev. B **4**, 1094 (1971).

³S. Zirinsky, Acta Met. **4**, 164 (1956).

⁴Y. Murakami, J. Phys. Soc. Jap. **33**, 1350 (1972).

⁵D. B. Novotny and J. F. Smith, Acta Met. **13**, 881 (1965).

⁶A. L. Tichener and M. B. Bever, Trans. AIME **200**, 303 (1954).

⁷D. B. Masson and C. S. Barrett, Trans. AIME **212**, 260 (1958).

⁸W. J. Buehler, J. V. Gilfrich, and R. C. Wiley, J. Appl. Phys. **34**, 1475 (1963).

⁹D. P. Dunne and C. M. Wayman, Met. Trans. **4**, 137 (1973).

¹⁰R. Smith and J. S. Bowles, Acta Met. **8**, 405 (1960).

¹¹L. Kaufman and M. Cohen, Progr. Metal Phys. **7**, 165 (1958).

¹²I. Cornelis, R. Oshima, H. C. Tong, and C. M. Wayman, presented at the American Society for Metals Fall Meeting, Chicago, Illinois, 1-4 October 1973 (unpublished).

¹³H. C. Tong and C. M. Wayman, Acta Met. **21**, 1381 (1973).

¹⁴A crystallographically equivalent distortion with expansion axis at 90° from that shown has been ignored for simplicity. This would result in an additional potential well to the left of D in Fig. 3(b) which would affect the transition time, but not by an order of magnitude.

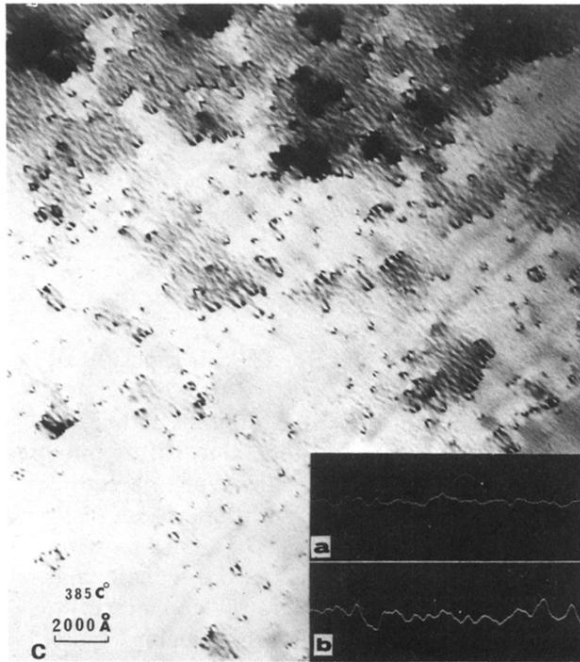


FIG. 1. (a) Background noise from 100-kev electron beam and electron multiplier. (b) Fluctuations in electron multiplier signal which correspond to pretransformation phenomena. The electron current input is the same as for (a) and the horizontal scale is 0.2 sec/cm. (c) Electron micrograph showing streaminglike lattice oscillations in CuAu alloy during pretransformation period.

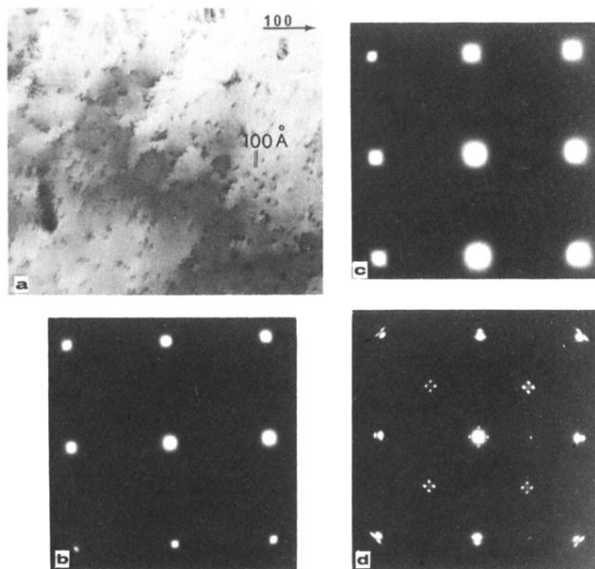


FIG. 2. (a) Transmission electron micrograph of CuAu thin film taken just before incipient transformation at 385°C ($\text{fcc} \rightarrow \text{CuAu II}$) showing the appearance of gridlike domain structure. (b) Diffraction pattern of CuAu film taken at 600°C showing sharp maxima. (c) Diffraction pattern of CuAu film taken at 385°C before transformation showing diffuse intensity and broadening of maxima caused by lattice oscillations. (d) Diffraction pattern of transformed CuAu thin film taken at 385°C showing sharp diffraction maxima.